Intensification of UV-C tertiary treatment: disinfection and removal of micropollutants by sulfate radical based Advanced Oxidation Processes

J. Rodríguez-Chueca[1, 2], C. García-Cañibano[1], R.-J. Lepistö[3], Á. Encinas[4], J. Pellinen[3], J. Marugán[1,*]

[1] Department of Chemical and Environmental Technology, ESCET, Universidad Rey Juan Carlos, C/ Tulipán s/n, 28933, Móstoles, Madrid, Spain. javier.marugan@urjc.es

[2] Department of Chemical and Environmental Engineering, Technical University of Madrid, (UPM), C/ José Gutiérrez Abascal 2, 28006, Madrid, Spain.

[3] Department of Environmental Sciences, University of Helsinki, Niemenkatu 73, FI-15140 Lahti, Finland.

[4] Department of Innovation & Technology, FCC Aqualia, S.A., C/ Montesinos 28, 06002, Badajoz, Spain.

*Author to whom correspondence should be addressed:

Tel: + 34 91 664 74 66; Email: javier.marugan@urjc.es

ABSTRACT

This study explores the enhancement of UV-C tertiary treatment by sulfate radical based Advanced Oxidation Processes (SR-AOPs), including photolytic activation of peroxymonosulfate (PMS) and persulfate (PS) and their photocatalytic activation using Fe(II). Their efficiency was assessed both for the inactivation of microorganisms and the removal or micropollutants (MPs) in real wastewater treatment plant effluents. Under the studied experimental range (UV-C dose 5.7 to 57 J/L; UV-C contact time 3 to 28 s), the photolysis of PMS and PS (0.01 mM) increased up to 25% the bacterial removal regarding to UV-C system. The photolytic activation of PMS led to the total inactivation of bacteria ($\approx$ 5.70 log) with the highest UV-C dose (57 J/L). However, these conditions were insufficient to remove the MPs, being required oxidant's dosages of 5 mM to remove above 90% of carbamazepine, diclofenac, atenolol and triclosan. The best efficiencies were achieved by the combination of PMS or PS with Fe(II), leading to the total removal of the MPs using a low UV-C dosage (19 J/L), UV-C contact time (9 s) and reagent's dosages (0.5 mM). Finally, high mineralization was reached (>50%) with photocatalytic activation of PMS and PS even with low reagent's dosages.
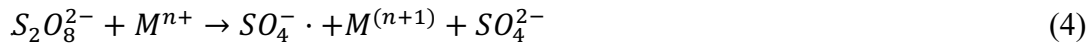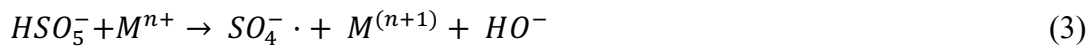
Keywords: SR-AOPs; UV-C; disinfection; micropollutants; real wastewater.

1.   Introduction

Water quality is currently threatened by micropollutants (MPs) detected at trace levels in water bodies and whose impact in the environment is of growing concern [1, 2]. These MPs originates from human activities such as farms, industries, hospitals and even domestic wastewaters [3, 4]. The detection of MPs in surface waters confirms that their removal efficiency in wastewater treatment plants (WWTP) is not complete [4, 5], due to their high chemical stability or low biodegradability [6]. The reach of groundwater and drinking water supplies is a serious threat for population, so it is crucial to develop efficient degradation strategies.

The intensification of tertiary treatments of wastewater is an alternative to achieve the degradation of MPs. Besides, the regeneration of wastewater is a solution to increase the water resources in regions with problems of water shortage. During the last decades, different international institutions (WHO, USEPA, etc.) and governments have published guidelines and laws to reuse reclaimed wastewater [7-9]. In Spain, the Royal Decree 1620/2007 establishes the maximum admissible values for different parameters as a function of the final use of reclaimed water [10]. The highest risk comes from biological agents causing waterborne diseases. Although conventional disinfectants as chlorination are very efficient, the generation of toxic disinfection by-products (DBPs) [11] has recently become a matter of concern among water utilities and regulators. Other efficient alternatives like UV-C lamps present problems of microbial regrowth, as they lack of residual effect and microorganisms have DNA repair mechanisms [12, 13]. For all these reasons, Advanced Oxidation Processes (AOPs) have been demonstrated as a promising technology to disinfect and remove MPs in a large extent [14-20].

AOPs involve *in-situ* generation of highly reactive free radicals, such as hydroxyl (HO·; HR-AOPs) or sulfate (SO4⁻·; SR-AOPs). This research explores the efficiency of different SR-AOPs in the disinfection and removal of MPs present in real secondary effluents. Sulfate radicals processes are based on the addition of persulfate salts, such as $Na_2S_2O_8$ and $KHSO_5$ [21]. Sulfate radicals (SO4⁻·) can be generated under different activation routes (reactions 1–4), such as UV, heat, high pH, and transition metal ions [22–30].

$$HSO_5^- \xrightarrow{h\nu/\Delta} SO_4^- \cdot + HO \cdot \qquad (1)$$

$$S_2O_8^{2-} \xrightarrow{h\nu/\Delta} 2SO_4^{2-} \cdot \qquad (2)$$

$$HSO_5^- + M^{n+} \rightarrow SO_4^- \cdot + M^{(n+1)} + HO^- \qquad (3)$$

$$S_2O_8^{2-} + M^{n+} \rightarrow SO_4^- \cdot + M^{(n+1)} + SO_4^{2-} \qquad (4)$$

On the other hand, the photolysis of H_2O_2 generates hydroxyl radicals (HR-AOP) when it is irradiated by photons of wavelengths lower than 300 nm (reaction 5):

$$H_2O_2 \xrightarrow{h\nu} 2HO \cdot \qquad (5)$$

UV/H_2O_2 process has been proven to be effective for the disinfection of microorganisms, control and treatment of trace organic contaminants [31–32]. Moreover, the second order rate constant of the reaction of sulfate and hydroxyl radicals with some MPs has been reported to be of the same order of magnitude [33].

This work presents a novel study on the disinfection and removal of MPs present in real secondary WWTP effluents via SR-AOPs. Treatment was carried out under very realistic conditions of continuous operation mode with contact time of few seconds to reproduce the operation of UV-C processes at industrial level. Different wastewater flow rates, oxidant and Fe(II) concentrations were tested with the objective to establish the optimal

conditions for disinfection and remove these MPs. The efficiency of these treatments is compared with the photolysis of H_2O_2 as HR-AOPs model.

2. Materials and methods

2.1. Water

Two different types of water were used: a) simulated urban wastewater (SWW), used as model water for the optimization of operating conditions; and, b) real urban wastewater (RWW) whose main physico-chemical parameters are shown in Table 1. RWW came from Estiviel WWTP, located in Toledo (Spain) and operated by FCC Aqualia. RWW were collected from the inlet of the UV-C system of the tertiary treatment in an intermediate bulk container (IBC), and shipped to Universidad Rey Juan Carlos (Móstoles, Spain), to do their characterization and the experimental treatments. Three different sampling campaigns were carried out between October of 2016 and March of 2017.

2.2. Chemicals

The SWW composition is as follows: meat peptone (Scharlab; 160 mg/L), meat extract (Scharlab; 110 mg/L), urea (Scharlab; $CO(NH_2)_2$; 30 mg/L), NaCl (Scharlab; 7 mg/L), $CaCl_2 \cdot 2H_2O$ (Scharlab; 4 mg/L), $MgSO_4 \cdot 7H_2O$ (Scharlab; 2 mg/L) and K_2HPO_4 (Scharlab; 28 mg/L) [34].

Photolytic and catalytic activation of potassium peroxymonosulfate ($2KHSO_5 \cdot KHSO_4 \cdot K_2SO_4$, PMS, Merck) and sodium persulfate ($Na_2S_2O_8$, PS, Scharlab) were applied using concentrations ranging from 0.01 to 5 mM. For catalytic activation of PMS and PS, Iron (II) sulfate heptahydrate ($FeSO_4 \cdot 7H_2O$, Panreac) was used, always in the same molar ratio than persulfate salts (1:1). Finally, H_2O_2 (HP, 30% w/w, Panreac) was used for application of H_2O_2/UV-C treatments. All the reagents used were analytical grade. Deionized water was used to prepare the SWW samples, being a compromise

between realistic water matrices with organic content competing for the oxidants and a constant water composition to guarantee reproducibility and comparability among the different processes.

2.3. Bacterial analyses

E. coli and *E. faecalis* were selected as model microorganisms due to their wide use as faecal contamination indicator. *E. coli* strain K12 and *E. faecalis* were provided by the Colección Española de Cultivos Tipo (CECT 4624 and CECT 5143 respectively). They were used to prepare the microbial suspensions spiked in the SWW samples. Fresh liquid cultures were prepared in Luria-Bertarni broth (Scharlau) and incubated at 37°C in a rotary shaker (150 r.p.m.) for 22h. Microbial suspensions were harvested by centrifugation at 3500 r.p.m. for 25 min. The microbial pellet was re-suspended in sterilized saline solution (NaCl 0.9%) and diluted in the reactor to an initial concentration of 10^6 CFU/mL.

The analyses of the microorganisms *E. coli* and *E. faecalis* were performed by the spread plate method after a serial 10-fold dilution in sterilized saline solution (NaCl 0.9%). Aliquots of diluted samples were plated on MacConkey Agar (Scharlau) for *E. coli* and Slanetz&Bartley agar (Scharlau) for *Enterococcus* sp. Colonies of *E. coli* and *Enterococcus* sp. were counted after 24h of incubation at 42ºC and 48h at 37ºC respectively. Additionally, fungi population was also followed in experiments with RWW. This analysis was also performed by the spread plate method, using Yeast Malt Extract Agar (Scharlau). Colonies were counted after incubation of 48h at 37ºC. RWW samples were not inoculated, and wild strains of microorganisms were analysed.

Microbial regrowth was estimated after the storage of the samples at room temperature for 24 and 48h, after the last sampling time.

2.4. Micropollutants analyses

The analytical methodology developed for the quantification of MPs is based on conventional solid phase extraction (SPE) followed by reverse phase liquid chromatography (UPLC) of the extract and detection by time-of-flight mass spectrometry (TOF-MS) (see supplementary material).

2.5. UV-C photoreactor

The system consists of a feed tank, a centrifugal pump and a rotameter at the inlet of the reactor. All the treatments were performed at the natural pH of samples without further adjustment (pH_{SWW} = 7.10; pH_{RWW} = 7.23) in continuous mode, with four different flow rates (1-10 L/min). No significant pH changes were recorded along the process, in agreement with other authors [35]. The reactor is a 46 cm in length and 3.60 cm in inner diameter quartz tube illuminated by a UV-C lamp (Philips TUV PL-L 95W/4P HO 1CT/25, λ_{max}=254 nm) placed 10 cm above the tube in the axis of a parabolic reflector. The total illuminated volume is ca. 470 mL. The UV-C contact time ranged from 2.8 to 28 s, and the UV-C dosages from 5.7 to 57 J/L, calculated from the experimental value of 95.5 W/m^2 measured with a UV-C radiometer (Delta OHM, Model HD 2102.2).

Experiments started when UV-C radiation was switched on, also corresponding to the simultaneous addition of oxidants and catalyst. During the course of the reaction, samples were collected at periodic intervals until steady-state was reached. All assays were carried out in triplicates, and results are presented as average data. For clarity purposes, error bars are not represented in all the figures, but the observed standard deviation was always less than 5% of the reported value.

3. Results and discussion

3.1. Optimization of operating conditions. Simulated wastewater disinfection

Different treatments were applied using SWW to optimize the operating conditions, taking as reference parameters the removal of bacteria population. Figure S1 (Supplementary Material) shows the effect of persulfate salts themselves over bacteria population in dark conditions. Oxidant's doses higher than 0.1 mM lead to bacterial inactivation in the dark. Therefore, 0.01 mM was chosen as oxidant dose for all the treatments, in order to ensure the photoactivated nature of the process, and to reduce costs.

Photolysis of PMS, PS and HP

Figure 1 shows the inactivation results for *E. coli* (Figure 1a) and *E. faecalis* (Figure 1b) obtained after the application of UV-C alone and in the presence of a low oxidants's dosage (0.01 mM). As expected, the highest inactivation was obtained with the highest UV-C contact time, 28 sec (1 L/min; UV-C dose 57 J/L). As observed, the addition of the oxidants enhanced significantly the disinfection. In the case of *E. coli*, from 3.50 log obtained only using UV-C, until values ranging 4.50–5 log after the addition of the oxidants. The differences between treatments are lower for *E. faecalis*, reaching inactivation values slightly higher than 3.50 log. Nevertheless, the largest efficiencies were observed for PMS in both cases, reaching inactivation values around 5-log. This value supposes an increase in efficiency of 43% regarding to UV-C treatments without oxidants. The higher efficiency of PMS could be attributed to its higher oxidant potential (E^o = 2.51 V) in comparison with PS (E^o = 2.01 V).

Figure 1 (a, b)

It is worth noting that the UV-C dose and UV-C contact time are common in real WWTP. For instance, the average UV-C dose and contact time in Estiviel WWTP, are in the order of 60 J/L and 7 seconds respectively, being enough to comply with the Spanish legislation of wastewater reuse (RD 1620/2007) [10]. This dose value is closer to the one corresponding to a flow rate of 10 L/min. It can be observed in the Figure 1, that for lower UV-C doses there are almost no differences in the bacterial efficiency when oxidants were added in comparison with UV-C alone. Only when HP was added, it was observed a slight increase in bacteria removal. In the case of *E. coli* (Figure 1a) it was observed as all the oxidants combined with UV-C, reached similar efficiency ranging from 2.5 to 3-log at 5 L/min (6 seconds UV-C contact time), when UV-C treatments reached only 1-log. Even when the highest flow rate was applied (3 seconds UV-C contact time) the addition of oxidants increased the efficiency significantly until 1.5–2-log. This behavior was observed in the case of *E. faecalis* as well (Figure 1b), however the efficiency gap is considerably lower than the observed for *E. coli*.

Metal activation of PMS and PS

The sulfate radicals generation rate could increase using a transition metal as activator of PMS and PS. While silver ion was proved to be the most efficient for activating the PS [26], for PMS activation, cobalt ion (Co^{2+}) exhibited the best activated performance [36]. The vast majority of authors agree that Co(II) and Fe(II) are the most suitable activators [26–31]. However, the environmental and health drawbacks of Co(II) dissuade their use, and for this reason this research only show the use of Fe(II) as activator.

Figure 2, shows the inactivation results of *E. coli* and *E. faecalis* (Figures 2a and 2b respectively) reached combining 0.01 mM of PMS and Fe(II) in the same molar ratio (1:1) irradiated with UV-C.

It can be clearly observed as the addition of Fe(II) enhanced the treatments PMS/UV-C and UV-C, reaching the total inactivation of *E. coli* (≈ 5.70-log) with 28 seconds of contact time. Although the reduction of *E. coli* population was lower when the flow rate was increased, it can be observed that the removal is higher than obtained with PMS/UV-C. Worth mentioning is the inactivation of *E. coli* (2.1-log) obtained with a flow rate of 10 L/min (3 seconds of UV-C contact time).

In the case of *E. faecalis*, the behavior is slightly different at high flow rates. At 1 L/min, the addition of Fe(II) increased the removal of *E. faecalis* until 5.5-log, higher than the removal with PMS/UV-C. However, because of the higher resistance of this bacteria, it can be observed in the figure as the addition of Fe(II) with high flow rates does not have effect in the activation of PMS. The inactivation differences between *Escherichia coli* and *Enterococcus faecalis* are related to the structural differences of both bacteria, usually being *E. faecalis* more resistant than *E.coli* [17].

Figure 2 (a, b)

The activation of persulfate salts (PMS and PS) has been widely reported in the literature for organic compounds removal [37–40], but to the best of our knowledge the number of references using these systems for water disinfection is much lower [41, 42]. In all the cases, the authors reported the efficiency in discontinuous mode, while this manuscript proved the efficiency in realistic conditions of continuous mode using very low UV-C contact time, and low reagent's dosages. Previous investigations have successfully applied this process to the disinfection of winery wastewater [41]. In this case, tenfold

PMS concentration was applied in batch mode and using UV-A LED radiation (370 nm), because of the much higher organic carbon load ($\approx$ 600 mg/L). Now, the current research shows the potential of this technology in the treatment of effluents at large scale in continuous mode, reducing the dosage of reagents, treating large water volumes. However, an important limitation is observed in the treatment, as the combination PMS/Fe(II)/UV-C only worked properly with the lowest flow rate. When flow rate is increased, the addition of Fe(II) did not improve the inactivation reached by PMS/UV-C. It seems that the contact time is not enough for reacting PMS and Fe(II), and the generation of radicals is similar that the obtained without Fe(II). Although the coupling of PMS/Fe(II) is one of the most common combination, it presents some disadvantages similar to the Fenton reaction, such as a slow regeneration of Fe(II) from Fe(III) and the production of a ferric hydroxide sludge [43].

On the other hand, the disinfection efficiency of coupling PS with Fe(II) and irradiation with UV-C (Figures 3a and 3b) was tested, adding the same molar concentration, 0.01 mM. Contrary to what happened in the case of PMS/Fe(II)/UV-C treatments, the combination coupling photocatalytic activation of PS by Fe(II) did not improve the inactivation results without Fe(II). For example, in the case of *E. coli* it can be observed that the efficiency of both treatments, with and without Fe(II) is similar for all the tested flow rates, suggesting that the applied operating conditions are not enough to enable significantly the catalytic activation of PS. Other authors reported the successful photocatalytic activation of PS using Fe(II) on the removal of organic pollutants [44], but with higher oxidant dosages and UV contact time.

Figure 3 (a, b)

3.2.   Disinfection and MPs removal of real wastewater

After reaching the optimal operating conditions to achieve total disinfection of wastewater, the efficiency of the processes was tested on RWW, in order to assess their possible application at full-scale. In this case, the effectiveness was studied not only over microbial population, but also in the more challenging goal of MPs removal.

Wastewater characterization. MPs occurrence

Table 2 shows the occurrence of some of the targeted MPs in RWW. As it can be observed, seven out of eleven different contaminants were detected (SCL, CFN, SMX, CBZ, ATN, DCF, TCS) at trace level (µg/L). The highest detected concentration corresponds to sucralose (SCL), ranging 20-24 µg/L. The use of sucralose has increased in the last decades in a vast variety of diets, as an important type of food additive. Other authors have reported similar values in groundwater and wastewater [45]. The concentration of the other MPs is ranging 0.1-1.2 µg/L. These values are similar than other reported by Collado et al. [4], in the characterization of different WWTP effluents. Some substances were not detected, such as SMZ, ATZ (both banned in Spain) and IBP. In the case of the IBP, despite its common presence in urban wastewaters, this substance is easily degraded in conventional WWTP, as reported by other authors [46–48].

Disinfection of treated wastewater effluents

Figure 4 shows the inactivation results of *E. coli*, *E. faecalis* and fungi population using 0.01 mM of reagent's dose. As observed in the Figure 4, because of the low microbial concentration in the samples, 10^2-10^4 CFU/100mL, almost all the applied treatments reached the detection limit (DL) of microbial determination at 1 and 3 L/min. For this reason, the comparison between the different treatments is performed in the highest flow rates (5 and 10 L/min). Figure 4a shows as the addition of low dosages of oxidants,

increased the bacteria inactivation regarding to the treatment using only UV-C. Therefore, UV-C alone reached *E. coli* inactivation of 0.80-log, while the highest inactivation value was obtained with the PS/UV-C treatment, reaching 2.08-log with a UV-C contact time of 6 seconds. This treatment was more efficient than the use of PMS and HP, even higher than coupled with Fe(II). In the case of *E. faecalis* (Figure 4b.) it is required to compare the results at 10 L/min. The highest efficiency was reached using HP/UV-C (1.22-log), more than 90% *E. faecalis* removal, just in 3 seconds with an UV-C dosage of 5.7 J/L. Fungi inactivation are shown in the Figure 4c. Fungi are eukaryotic cells with different resistance, so their use as biological control parameter could provide useful and reliable information about the treatments efficiency. As shown in the figure, the low dosage of reagents enough for bacteria inactivation is not suitable for fungi. Again, it is observed as the addition of oxidants improved significantly the fungi inactivation regarding to UV-C alone, mainly at 1 and 3 L/min, reaching the detection limit with HP/UV-C, and values higher than 3-log with photolysis of PMS and PS, when 1 L/min was used, and higher than 2-log at 3 L/min. Nevertheless, using even higher flow rates, only PMS/UV-C and PS/UV-C obtained a disinfection higher than 1-log. Therefore, the SR-AOPs applied in this research, and specially PMS/UV-C and PMS/Fe(II)/UV-C, are more efficient in the disinfection of wastewater with a high microbial load ($>10^6$ CFU/mL) than UV-C alone. With low microbial loads, UV-C radiation is enough to reach the highest disinfection level requited by the Spanish Legislation about reuse of reclaimed wastewater (RD 1620/2007) [10].

<u>Figure 4</u>

Photolytic activation of PMS and PS

Table 3 shows the degradation results of the detected MPs after the application of H_2O_2/UV-C, PMS/UV-C and PS/UV-C at 1 and 3 L/min increasing oxidant dosages (0.05-5 mM). The conditions used for disinfection (0.01 mM as reagents dosage) were insufficient to improve UV-C radiation effect on the removal of MPs (data not shown). Actually the lowest concentration shown in Table 3 (0.05 mM) is still not enough for significantly improving the efficiency of UV-C radiation alone, although there are some exceptions. For instance, 0.05 mM PS/UV-C enhance the efficiency of UV-C on the removal of ATN and DCF, reaching 37 and 39%, respectively at 1 L/min.

Very high removal efficiency was reached for three pollutants (94% DCF; 95% ATN; 74% TCS), by applying PS/UV-C treatment at 1 L/min using the intermediate dosage of 0.5 mM. Using shorter contact time led to lower efficiencies, as expected from the lower UV-C dosage, although in the case of ATN a high efficiency is also obtained at 3 L/min. Nevertheless, the best removal efficiency is obtained with the highest dosage (5 mM) in almost all the compounds. Removals above 95% are obtained for CBZ, DCF, ATN and TCS (in some cases 100%), by using photolytic activation of the highest concentration of persulfate salts (PMS and PS) at 1 L/min. Even at 3 L/min some of them show removal efficiencies higher than 90%, in the case of DCF with both SR-AOPs, but CBZ just by PMS/UV-C, and TCS by PS/UV-C. In all the studied situations, the treatments based on sulfate radicals provided higher results than photolysis of H_2O_2, whose best results were removals above 50% (56% CBZ; 57% DCF; 56% ATN; 65% TCS).

Despite the previous results, the applied treatments did not work satisfactorily for all the compounds, such as the case for SMX and SCL. For SMX, 5 mM PS/UV-C treatments reached some removal (47±1%) at 1 L/min, but unfortunately the rest of the treatments

did not work. In the case of SCL, the most efficient treatment was 5 mM H_2O_2/UV-C, but the removal only slightly exceeds 20%. Finally, CFN was detected in low concentration in the raw wastewater, with values below quantification limit, and was not detected at the outlet of the treatments.

Some authors have studied the removal of MPs by the application of these treatments at lab-scale in batch reactors. Xu et al. [50] reported the total removal of SCL after 60 minutes of reaction by 3.78 mM PMS/UV-C. This result contrast with the reported in this study (13% using 5 mM PMS/UV-C), but in this case the UV-C contact time corresponds with 28 s and SCL is presented in a very complex real WWTP effluent. Shukla et al. [51] reported the use of PMS, PS and HP in combination with UV-C for the removal of phenolic contaminants. After 350 minutes of reaction, total removal of phenol was reached with PS/UV-C and HP/UV-C with dosages below $7.0 \cdot 10^{-3}$ mM. Sharma et al. [52] reported the 96.7% removal of Bisphenol A under 360 minutes of 0.66 mM PMS/UV-C. Luo et al. [53] reported that PS/UV-C system is more effective than PMS/UV-C and HP/UV-C for degradation of ATZ. This conclusion fits with the results shown in this manuscript. On the other hand, Pablos et al. [40] showed some extent removal of different MPs during HP/UV-C disinfection treatments carried out in a closed recirculating annular reactor. With an initial amount of 100 mg/L of HP, almost 50% of SMX removal was obtained after 60 min. Although, the results presented in this report cannot be compared with the ones obtained by the above mentioned authors [40, 50-53], they gain relevance considering the realistic conditions of contact time (28 s) and WWTP effluents for the industrial application of these processes.

Iron (II) catalytic activation of PMS and PS

Table 4 shows the MPs removal efficiency of Fe(II) catalytic activation of PMS and PS using different reagent's dosages at 1 and 3 L/min. An optimal molar ratio ratio 1:1 Oxidant:Fe(II) was established based on preliminary experiments.

As previously observed in Table 3, photolytic activation of PMS and PS reached the total removal of some MPs with 5 mM dosages. Therefore, it only makes sense to add iron to improve the efficiency for lower reagent's dosages. For example, in the cases of DCF and ATN using the lowest dosage of PMS (0.05 mM), the addition of Fe(II) significantly improved the efficiency reached in absence of Fe(II). Nevertheless, the effect of the combination of Fe(II) with persulfate salts can be better verified using the intermediate reagent's concentration. In this case, CBZ, DCF, ATN and TCS were removed higher than 75%, even at 3 L/min. Even ATN reached 100% of removal in all the studied scenarios. There are not significant differences between the use of PMS and PS in combination with Fe(II), just in the case of SMX (60% with PMS; 100% with PS). Finally, the combination of PS with Fe(II) using the highest concentration of the reagents was useful to abate SCL in a high extent (50%).

The differences in the removal efficiency of the different MPs should be related to their specific structure and chemical composition (i.e. functional groups) and their physicochemical properties that makes them more or less refractory to the attack of the oxidant species. As an example, Luo et al. [49] classified the potential removal of hydrophilic micropollutants by sorption according to the value of the partition coefficient, $logK_{ow}$. Table S1 (Supplementary material) shows the structure and physicochemical properties of the micropollutants detected in the wastewater samples. According to Table S1, CBZ, CFN, SMX, ATN and SCL present a higher hydrophilicity. However, it is not

obvious the existence of a relation exist with the removal efficiency, being CFN and ATN poorly removed by the same treatments, whereas both present completely different values of hydrophilicity. No clear relation can be neither derived between the chemical structure and functional groups of the compounds (shown in Table S1) and their removal efficiencies. Therefore, until a much deeper knowledge of the relation between chemical structure and physicochemical properties of the MPs enables the prediction of the efficiencies, an experimental approach based on the huge amount of scientific data reported in the literature should be adopted for the design of the removal treatments.

The efficient activation of PMS and PS through the use of different transition metals, mainly iron, has been reported in literature [53-55]. For example, Ahmed and Chiron [55] proved PS/Fe(II)/UV–Vis using solar irradiation, and they reported the efficiency improvement for CBZ abatement regarding to PS/Fe(II) and PS/UV–Vis. They found 2:1 as optimal molar ratio PS:Fe(II) for a full mineralization of CBZ in 30 min with a CBZ:PS ratio of 1:40.

In terms of mineralization, Table 5 shows the DOC removal. The highest DOC abatement are observed for PS/UV-C in almost all the cases, with values around 50%. On the other hand, although H_2O_2/UV-C did not reach high levels of MPs removal, the DOC abatement is higher than the obtained with PMS/UV-C. The addition of Fe(II) increased the mineralization, reaching values higher than 50% in all the cases, with the highest values correspond to PMS/Fe(II)/UV-C. Assuming that the reported data can be extrapolated to the MPs, these high mineralization rates are definitively a promising result, although further studies are indeed needed to examine the oxidation by-products generated after these UV-C-based AOPs.

4. Conclusions

This work demonstrated the efficiency of SR-AOPs to intensify UV-C tertiary treatments to remove completely the biological load and MPs detected in real secondary effluents using very low reagent's doses (0.5 mM) and very low UV-C contact time (9 seconds). Lower dosages (0.01 mM) were enough to inactivate microbial populations completely, but insufficient to degrade MPs.

Application of SR- and HR-AOPs significantly improves the efficiency of UV-C on the removal of MPs detected at trace level in WWTP effluents. Both PMS/UV-C and PS/UV-C showed better performance than HP/UV-C. In general, the addition of Fe(II) as catalyst for PMS and PS activation allows reaching a complete removal of the MPs even using a very low UV-C dosage of 19 J/L, corresponding to a short UV-C contact time of 9 s, and reduced reagent's dosages (0.5 mM). Even though the latter was the general case, some MPs such as SCL, could not be removed satisfactorily, reaching only 50% of removal even under the strongest conditions (5 mM PS/Fe(II)/UV-C at 1 L/min; 57 J/L; 28 s). Although further studies are needed to elucidate the by-products generated after these UV-C-based AOPs, the high mineralization (> 50%) reached by the PMS/Fe(II)/UV-C and PS/Fe(II)/UV-C even with low reagent's dosages might open new remediation strategies for the removal of MPs in the tertiary treatment of WWTP effluents. This would allow the reuse of wastewater according to Spanish legislation (RD 1620/2007) without risk of bacterial regrowth.

Acknowledgements

References

[1] I. Michael, L. Rizzo, C.S. McArdell, C.M. Manaia, D. Fatta-Kassinos, Urban wastewater treatment plants as hotspots for the release of antibiotics in the environment: A review, Water Res. 47(3) (2013) 957-995.

[2] K.K. Philippe, R. Timmers, R. van Grieken, J. Marugan, Photocatalytic disinfection and removal of emerging pollutants from effluents of biological wastewater treatments, using a newly developed large-scale solar simulator, Ind. Eng. Chem. Res. 55 (2016) 2952−2958.

[3] C.G. Daughton, T. Ternes, Pharmaceuticals and personal care products in the environment: agents of subtle change? Environ. Health Perspect. 107 (1999) 907–938.

[4] N. Collado, S. Rodriguez-Mozaz, M. Gros, A. Rubirola, D. Barceló, J. Comas, I. Rodriguez-Roda, G. Buttiglieri, Pharmaceuticals occurrence in a WWTP with significant industrial contribution and its input into the river system, Environ. Pollut. 185 (2014) 202–212.

[5] M.S. Kostrich, A.L. Batt, J.M. Lazorchak, Concentrations of prioritized pharmaceuticals in effluents from 50 large wastewater treatment plants in the US and implications for risk estimation, Environ. Pollut. 184 (2014) 354–359.

[6] B. Halling-Sørensen, S.N. Nielsen, P.F. Lanzky, F. Ingerslev, H.C.H. Lützhøft, S.E. Jørgensen, Occurrence, fate and effects of pharmaceutical substances in the environment – a review, Chemosphere 36 (2) (1998) 357–394.

[7] USEPA (US Environmental Protection Agency) 2004. Guidelines for Water Reuse. USEPA, Washington, DC, USA.

[8] EPA (Environmental Protection Agency) (Queensland State) 2005. Queensland Water Recycling Guidelines. EPA, Brisbane, Australia, 2005.

[9] WHO 2006. Guidelines for the Safe use of Wastewater, Excreta and Greywater, Vol 1. WHO, Geneva, Switzerland.

[10] Royal Decree 1620/2007 (BOE No. 294, December 8, 2007. Concerns of the legal regime for the reuse of treated water. Available at: http://www.boe.es/boe/dias/2007/12/08/pdfs/A50639-50661.pdf.

[11] J.J. Rook, Formation of haloforms during chlorination of natural water, Water Treat. Exam. 23 (2) (1974) 234–243.

[12] K. Oguma, H. Katayama, H. Mitani, S. Morita, T. Hirata, S. Ohgaki, Determination of pyrimidine dimers in *Escherichia coli* and *Cryptosporidium parvum* during UV light inactivation, photoreactivation, and dark repair, Appl. Environ. Microb. 67 (2001) 4630–4637.

[13] H. Liltved, B. Landfald, Effects of high intensity light on ultraviolet-irradiated and non-irradiated fish pathogenic bacteria, Water Res. 34 (2000) 481–486.

[14] R. van Grieken, J. Marugán, C. Pablos, L. Furones, A. López, Comparison between the photocatalytic inactivation of Gram-positive *E. faecalis* and Gram-negative *E. coli*

faecal contamination indicator microorganisms, Appl. Cat. B: Environ. 100 (1–2) (2010) 212-220.

[15] P.S.M. Dunlop, M. Ciavola, L. Rizzo, J.A. Byrne, Inactivation and injury assessment of *Escherichia coli* during solar and photocatalytic disinfection in LDPE bags, Chemosphere 85 (7) (2011) 1160-1166.

[16] M.I. Polo-López, I. Oller, P. Fernández-Ibáñez, Benefits of photo-Fenton at low concentrations for solar disinfection of distilled water. A case study: *Phytophthora capsici*, Cat. Today 209 (2013) 181-187.

[17] J. Rodríguez-Chueca, M.I. Polo-López, R. Mosteo, M.P. Ormad, P. Fernández-Ibáñez, Disinfection of real and simulated urban wastewater effluents using a mild solar photo-Fenton, Appl. Catal. B. Environ. 150–151 (2014) 619-629.

[18] S. Giannakis, E. Darakas, A. Escalas-Cañellas, C. Pulgarin, Solar disinfection modeling and post-irradiation response of *Escherichia coli* in wastewater, Chem. Eng. J. 281 (2015) 588-598.

[19] S. Cotillas, M.J. Martín de Vidales, J. Llanos, C. Sáez, P. Cañizares, M.A. Rodrigo. Electrolytic and electro-irradiated processes with diamond anodes for the oxidation of persistent pollutants and disinfection of urban treated wastewater. J. Hazard. Mater. 319 (2016) 93-101.

[20] G. Ferro, F. Guarino, A. Cicatelli, L. Rizzo, β-lactams resistance gene quantification in an antibiotic resistant Escherichia coli water suspension treated by advanced oxidation with UV/H_2O_2, J. Hazard. Mater. 323 (Part A) (2017) 426-433.

[21] G. Wei, X. Liang, Z. He, Y. Liao, Z. Xie, P. Liu, S. Ji, H. He, D. Li, J. Zhang, Heterogeneous activation of Oxone by substituted magnetites $Fe_{3-x}M_xO_4$ (Cr, Mn Co, Ni) for degradation of Acid Orange II at neutral pH, J. Mol. Catal. A: Chem. 398 (2015) 86–94.

[22] P.D. Goulden, D.H.J. Anthony, Kinetics of uncatalyzed peroxydisulfate oxidation of organic material in fresh water. Anal. Chem. 50 (1978) 953-958.

[23] F. Nydahl, On the peroxodisulphate oxidation of total nitrogen in waters to nitrate. Water Res. 12 (1978) 1123-1130.

[24] S. Malato, J. Blanco, C. Richter, B. Braun, M.I. Maldonado, Enhancement of the rate of solar photocatalytic mineralization of organic pollutants by inorganic oxidizing species. Appl. Catal. B. Environ. 17 (1998) 347-356.

[25] R.E. Huie, C.L. Clifton, P. Neta, Electron transfer reaction rates and equilibria of the carbonate and sulphate radical anions, Int. J. Radiat. Appl. Instrum. C. Radiat. Phys. Chem. 38(5) (1991) 477–481.

[26] G.P. Anipsitakis, D.D. Dionysiou, Radical generation by the interaction of transition metals with common oxidants, Environ. Sci. Technol. 38 (2004) 3705–3712.

[27] O.S. Furman, A.L. Teel, R.J. Watts, Mechanism of base activation of persulfate, Environ. Sci. Technol. 44 (2010) 6423–6428.

[28] Y. Liu, X. He, Y. Fu, D.D. Dionysiou, Kinetics and mechanism investigation on the destruction of oxytetracycline by UV-254 nm activation of persulfate, J. Hazard. Mater. 305 (2016) 229–239.

[29] S. Khan, X. He, J.A. Khan, H.M. Khan, D.L. Boccelli, D.D. Dionysiou, Kinetics and mechanism of sulfate radical- and hydroxyl radical-induced degradation of highly chlorinated pesticide lindane in UV/peroxymonosulfate system, Chem. Eng. J. 318 (2017) 135–142.

[30] J. Rodríguez-Chueca, C. Amor, T. Silva, D.D. Dionysiou, G. Li Puma, M.S. Lucas, J.A. Peres, Treatment of winery wastewater by sulphate radicals: HSO_5^-/transition metal/UV-A LEDs, Chem. Eng. J. 310 (2) (2017) 473-483.

[31] S. Semitsoglou-Tsiapou, M. R. Templeton, N.J.D. Graham, L. Hernández Leal, B.J. Martijn, A. Royce, J.C. Kruithof, Low pressure UV/H_2O_2 treatment for the degradation of the pesticides metaldehyde, clopyralid and mecoprop – Kinetics and reaction product formation, Water Res. 91 (2016) 285–294.

[32] Z. Shu, A. Singha, N. Klamerth, K. McPhedran, J.R. Bolton, M. Belosevic, M.G. El-Din. Pilot-scale UV/H_2O_2 advanced oxidation process for municipal reuse water: Assessing micropollutant degradation and estrogenic impacts on goldfish (*Carassius auratus L.*). Water Res. 101 (2016) 157-166.

[33] Z. Yang, R. Su, S. Luo, R. Spinney, M. Cai, R. Xiao, Z. Wei, Comparison of the reactivity of ibuprofen with sulfate and hydroxyl radicals: An experimental and theoretical study, Sci. Total Environ. 590-591 (2017) 751-760.

[34] OECD Guidelines for Testing of Chemicals, Simulation Test-Aerobic Sewage Treatment 303A, 1999.

[35] H. Zhang, X. Liu, J. Ma, C. Lin, C. Qi, X. Li, Z. Zhou, G. Fan. Activation of peroxymonosulfate using drinking water treatment residuals for the degradation of atrazine, J. Hazard. Mater. 344 (2018) 1220-1228.

[36] P. Hu, M. Long. Cobalt-catalyzed sulfate radical-based advanced oxidation: A review on heterogeneous catalysts and applications, Appl Catal B 181 (2016) 103-117.

[37] P. Shukla, I. Fatimah, S. Wang, H. M. Ang, M. O. Tadé, Photocatalytic generation of sulphate and hydroxyl radicals using zinc oxide under low-power UV to oxidise phenolic contaminants in wastewater, Catal. Today 157 (2010) 410–414

[38] J. Sharma, I.M. Mishra, D. D. Dionysiou, V. Kumar, Oxidative removal of Bisphenol A by UV-C/peroxymonosulfate (PMS): Kinetics, influence of co-existing chemicals and degradation pathway, Chem. Eng. J. 276 (2015) 193–204.

[39] C. Luo, J. Ma, J. Jiang, Y. Liu, Y. Song, Y. Yang, Y. Guan, D. Wu, Simulation and comparative study on the oxidation kinetics of atrazine by UV/H_2O_2, UV/HSO_5^- and $UV/S_2O_8^{2-}$, Water Res 80 (2015) 99 – 108.

[40] C. Pablos, J. Marugán, R. van Grieken, E. Serrano, Emerging micropollutant oxidation during disinfection processes using UV-C, $UV-C/H_2O_2$, $UV-A/TiO_2$ and $UV-A/TiO_2/H_2O_2$, Water Res. 47 (3) (2013) 1237 – 1245.

[41] J. Rodríguez-Chueca, S.I. Moreira, M.S. Lucas, J.R. Fernandes, P.B. Tavares, A. Sampaio, J.A. Peres, Disinfection of simulated and real winery wastewater using sulphate radicals: Peroxymonosulphate/transition metal/UV-A LED oxidation, J. Clean. Prod. 149 (2017) 805-817.

[42] J. Rodríguez-Chueca, T. Silva, J.R. Fernandes, M.S. Lucas, G. Li Puma, J.A. Peres, A. Sampaio. Inactivation of pathogenic microorganisms in freshwater using HSO_5^-/UV-A LED and HSO_5^-/M^{n+}/UV-A LED oxidation processes, Water Res. 123 (2017) 113-123.

[43] Y.R. Wang, W. Chu, Photo-assisted degradation of 2,4,5-trichlorophenoxyacetic acid by Fe(II)-catalyzed activation of Oxone process: the role of UV irradiation, reaction mechanism and mineralization, Appl. Catal. B Environ. 123-124 (2012) 151-161.

[44] Y. Liu, A. Zhou, Y. Gan, X. Li, Roles of hydroxyl and sulfate radicals in degradation of trichloroethene by persulfate activated with Fe^{2+} and zero-valent iron: Insights from carbon isotope fractionation, J. Hazard. Mater. 344 (2018) 98-103.

[45] W.D. Robertson, D.R. van Stempvoort, J. Spoelstra, S.J. Brown, S.L. Schiff, Degradation of sucralose in groundwater and implications for age dating contaminated groundwater, Water Res. 88 (2016) 653–660.

[46] C. Reyes-Contreras, M. Hijosa-Valsero, R. Sidrach-Cardona, J.M. Bayona, E. Bécares, Temporal evolution in PPCP removal from urban wastewater by constructed wetlands of different configuration: a medium-term study, Chemosphere 88 (2012) 161–167.

[47] S.K. Behera, H.W. Kim, J.E. Oh, H.S. Park, Occurrence and removal of antibiotics, hormones and several other pharmaceuticals in wastewater treatment plants of the largest industrial city of Korea, Sci. Total Environ. 409 (2011) 4351–4360.

[48] I. Martínez-Alcalá, J.M. Guillén-Navarro, C. Fernández-López, Pharmaceutical biological degradation, sorption and mass balance determination in a conventional activated-sludge wastewater treatment plant from Murcia, Spain, Chem. Eng. J. 316 (2017) 332–340.

[49] Y. Luo, W. Guo, H.H. Ngo, L.D. Nghiem, F.I. Hai, J. Zhang, S. Liang, X.C. Wang. A review on the occurrence of micropollutants in the aquatic environment and their fate and removal during wastewater treatment, Sci Total Environ 473-474 (2014) 619–641.

[50] Y. Xu, Z. Lin, Y. Wang, H. Zhang. The UV/peroxymonosulphate process for the mineralization of artificial sweetener sucralose, Chem. Eng. J., 317 (2017), 561–569.

[51] P. Shukla, I. Fatimah, S. Wang, H.M. Ang, M.O. Tadé, Photocatalytic generation of sulphate and hydroxyl radicals using zinc oxide under low-power UV to oxidise phenolic contaminants in wastewater, Catal. Today 157 (2010) 410–414.

[52] J. Sharma, I.M. Mishra, D.D. Dionysiou, V. Kumar, Oxidative removal of Bisphenol A by UV-C/peroxymonosulfate (PMS): Kinetics, influence of co-existing chemicals and degradation pathway, Chem. Eng. J. 276 (2015) 193–204.

[53] G.P. Anipsitakis, D.D. Dionysiou, Degradation of organic contaminants in water with sulfate radicals generated by the conjunction of peroxymonosulfate with cobalt, Environ. Sci. Technol. 37 (2003) 4790–4797.

[54] Y.R. Wang, W. Chu, Photo-assisted degradation of 2,4,5-trichlorophenoxyacetic acid by Fe(II)-catalyzed activation of Oxone process: the role of UV irradiation, reaction mechanism and mineralization, Appl. Catal. B Environ. 123–124 (2012) 151–161.

[55] M.M. Ahmed, S. Chiron, Solar photo-Fenton like using persulphate for carbamazepine removal from domestic wastewater, Water Res. 48 (2014) 229–236.

Figure captions

Figure 1. Comparison between (■) UV-C and photolysis of (●) PMS, (▲) PS and (▼) HP with UV-C treatments in the inactivation of (a) *Escherichia coli* and (b) *Enteroroccus faecalis*, using different flow rates (1, 3, 5 and 10 L/min). The time scale corresponds to the operation time of the continuous process required to achieve the steady state.

Figure 2. Efficiency of PMS activation with Fe(II) (▲), and comparison with (■) UV-C and photolysis of (●) PMS, in the inactivation of (a) *Escherichia coli* and (b) *Enteroroccus faecalis*, using different flow rates (1, 3, 5 and 10 L/min). The time scale corresponds to the operation time of the continuous process required to achieve the steady state.

Figure 3. Efficiency of PS activation with Fe(II) (▼), and comparison with (■) UV-C and photolysis of (▲) PS, in the inactivation of (a) *Escherichia coli* and (b) *Enteroroccus faecalis*, using different flow rates (1, 3, 5 and 10 L/min). The time scale corresponds to the operation time of the continuous process required to achieve the steady state.

Figure 4. Efficiency of different oxidation treatments in the inactivation of microorganisms of RWW samples: a) *Escherichia coli*; b) *Enterococcus faecalis*; c) fungi population. Operating conditions: [Oxidant] = 0.01 M; [Fe^{2+}] = 0.01 M; UV-C (95 W); continuous mode; FR = 1 – 10 L/min; UV-C contact time = 3 – 28 seconds.

Table captions

Table 1. Physico-chemical characteristics of wastewater during the three different campaigns (October '16 – March '17).

Table 2. Occurrence of MPs in real secondary effluents during three different campaigns in the period from October '16 to March '17 (concentration in µg/L).

Table 3. Percentage of MPs degradation by UV-C photolytic activation of HP, PMS and PS using different oxidant concentration at 1 L/min (28 sec UV-C contact time; UV-C dose: 57 J/L) and 3 L/min (9 sec UV-C contact time; UV-C dose: 19 J/L). The average and standard deviation of three replicates is given, except for the treatment with 0.05 mM reagent addition.

Table 4. Percentage of micropollutants degradation by catalytic activation of PMS and PS using Fe(II) and UV-C radiation, with different oxidant concentration at 1 L/min (28 sec UV-C contact time; UV-C dose: 57 J/L) and 3 L/min (9 sec UV-C contact time; UV-C dose: 19 J/L). The average and standard deviation of three replicates is given, except for the treatment with 0.05 mM reagent addition. DL is the detection limit, function of the initial concentration.

Table 5. Mineralization percentage of organic matter after the application of the treatments.

Table 1.

Parameter	October'16	January'17	March'17
pH	7.23 ± 0.12	7.30 ± 0.12	7.17 ± 0.08
Conductivity (μS/cm)	1330 ± 245	1110 ± 66	1040 ± 83
Turbidity (NTU)	4 ± 2	4 ± 1	4 ± 1
Suspended solids (mg/L)	10 ± 6	7 ± 3	5 ± 2
BOD (mg/L)	6 ± 1	6 ± 1	7 ± 2
COD (mgO$_2$/L)	28 ± 4	31 ± 3	27 ± 3
DOC (mg/L)	17 ± 4	15 ± 6	20 ± 8
Total Nitrogen (mg/L)	10 ± 2	11 ± 1	9 ± 1
Total Phosphorus (mg/L)	0.83 ± 0.29	0.79 ± 0.24	0.67 ± 0.14
Ammonia (mg/L)	1 ± 2	1 ± 1	0.70 ± 1
Nitrates (mg/L)	7 ± 2	9 ± 1	6 ± 1

Table 2

Group	Compound	October 2016	January 2017	March 2017
Analgesics and anti-inflammatories	DCF	1.22 ± 0.11	1.11 ± 0.05	0.96 ± 0.04
	IBP	n.d.	n.d.	n.d.
Antibiotics	SMX	0.50 ± 0.05	0.40 ± 0.03	0.41 ± 0.04
Psychiatric drugs	CBZ	0.72 ± 0.06	0.37 ± 0.03	0.22 ± 0.03
β-blockers	ATN	0.12 ± 0.02	0.15 ± 0.01	0.11 ± 0.03
Herbicides	SMZ	n.d.	n.d.	n.d.
	ATZ	n.d.	n.d.	n.d.
Anti-bacterials and Fungicides	TCS	0.16 ± 0.02	0.11 ± 0.01	0.06 ± 0.00
Stimulants	CFN	0.09 ± 0.12	0.07 ± 0.03	0.01
Sweeteners	SCL	23.80 ± 2.30	20.90 ± 1.40	20.00 ± 1.80

Table 3

Compound	[Reagent] mM	UV-C		HP/UV-C		PMS/UV-C		PS/UV-C	
		1 L/min	3 L/min	1 L/min	3 L/min	1 L/min	3 L/min	1 L/min	3 L/min
DCF	0.05			20	8	25	1	39	9
	0.5	32 ± 5	9 ± 6	40 ± 5	21 ± 1	56 ± 3	31 ± 2	94	26 ± 0
	5			57 ± 3	38 ± 2	100	100	96 ± 0	92 ± 3
SMX	0.05			0	0	0	0	0	0
	0.5	1 ± 0.41	0	10 ± 2	9 ± 4	0	0	44	0
	5			19 ± 2	12 ± 2	0	0	47 ± 1	0
CBZ	0.05			3	7	1	0	3	2
	0.5	10 ± 2	3 ± 4	31 ± 3	23 ± 8	23 ± 13	14 ± 3	26 ± 7	12 ± 4
	5			56 ± 3	44 ± 1	100	100	67 ± 16	39 ± 5
ATN	0.05			0	4	7	24	37	21
	0.5	5 ± 7	0	34 ± 2	28 ± 5	75 ± 4	69 ± 5	95 ± 6	59 ± 5
	5			56 ± 18	33	97 ± 6	88 ± 11	97 ± 4	81 ± 4
TCS	0.05			22	16	19	0	26	2
	0.5	34 ± 31	15 ± 26	40 ± 8	26 ± 6	28 ± 1	18 ± 7	74	10 ± 12
	5			65 ± 2	46 ± 1	100	24 ± 14	97 ± 5	100
SCL	0.05			0	8	2	0	7	7 ± 2
	0.5	8 ± 11	11 ± 13	9 ± 4	12 ± 8	9 ± 2	7 ± 2	36	0
	5			23 ± 3	20 ± 2	13 ± 2	6 ± 1	3 ± 1	0

Table 4

Compound	[Reagent] mM	Treatment			
		PMS/Fe(II)/UV-C		PS/Fe(II)UV-C	
		1 L/min	3 L/min	1 L/min	3 L/min
DCF	0.05	51	41	16	11 ± 1
	0.5	77 ± 16	96 ± 2	100	100
	5	100	100	100	98 ± 2
SMX	0.05	0	0	0	0
	0.5	67 ± 4	59 ± 3	100	0
	5	100	100	100	100
CBZ	0.05	11	9	12	13 ± 2
	0.5	86 ± 25	100	89 ± 15	78 ± 5
	5	100	100	100	100
ATN	0.05	46	38	1	0
	0.5	100 ± 0	100	100	100
	5	100	100	100	100
TCS	0.05	25	7	13	4
	0.5	100	97 ± 3	95 ± 6	88 ± 9
	5	100	100	100	100
SCL	0.05	8	10	0	3 ± 3
	0.5	21 ± 2	24 ± 2	6 ± 2	4 ± 4
	5	17 ± 5	13 ± 5	49 ± 1	24 ± 9

Table 5

Treatment	H$_2$O$_2$/UV-C	PMS/UV-C	PS/UV-C	PMS/Fe(II)/UV-C	PS/Fe(II)/UV-C
Dosage	Flow rate = 1 L/min				
0.05 mM	0	6 ± 3	2 ± 1	12 ± 4	10 ± 3
0.5 mM	37 ± 9	23 ± 2	27 ± 11	49 ± 2	54 ± 5
5 mM	45 ± 3	17 ± 1	54 ± 8	62 ± 3	44 ± 2
	Flow rate = 3 L/min				
0.05 mM	0	0	0	4 ± 2	4 ± 1
0.5 mM	9 ± 3	20 ± 8	47 ± 8	62 ± 7	51 ± 8
5 mM	38 ± 5	27 ± 1	51 ± 8	58 ± 1	3

Figure 1.
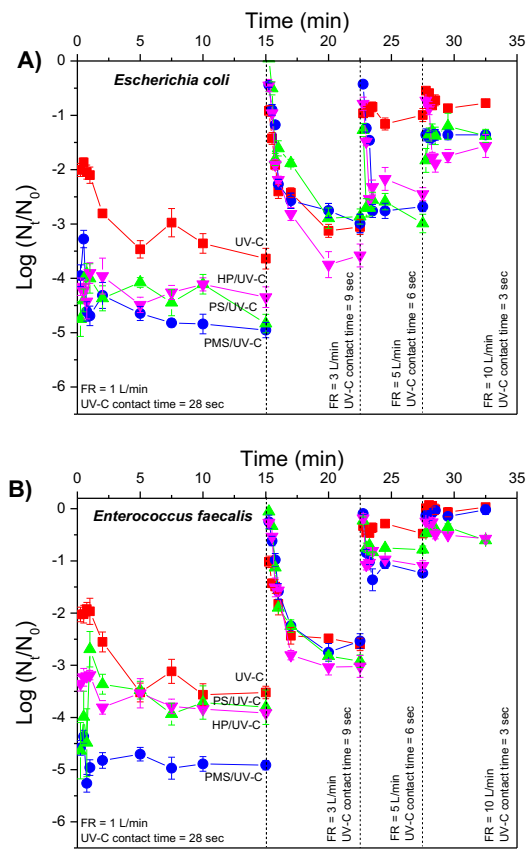
Figure 2.
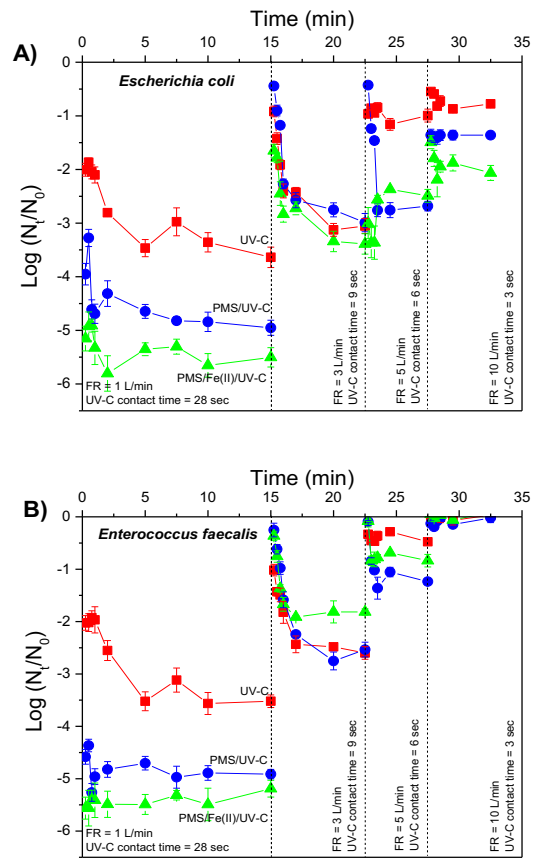
Figure 3.
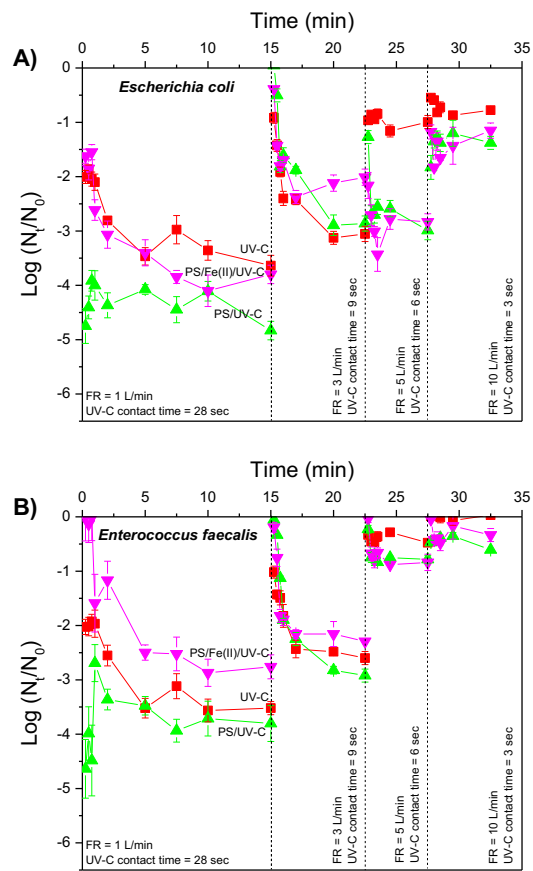
Figure 4.
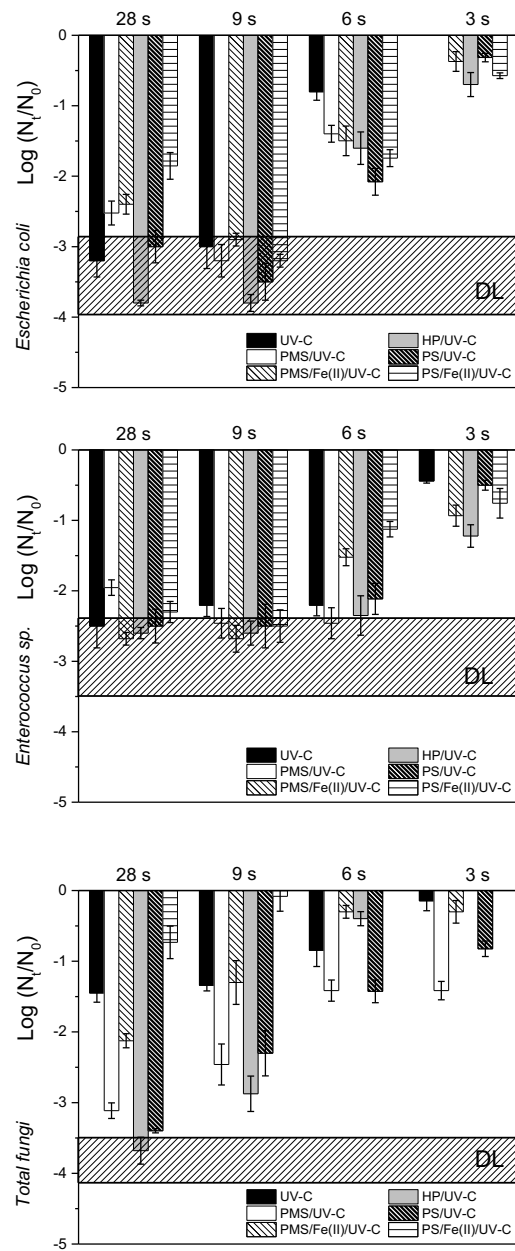
SUPPLEMENTARY MATERIAL

S1.   Micropollutants analyses

Solid Phase Extraction

An internal standard mixture was added to a filtered 100 mL water sample and the sample was extracted with a Waters Oasis HLB SPE cartridge that was first conditioned with 4 mL of methanol and 2x4 mL of water. The cartridge was then washed with 2x4 mL of 5% methanol in water and dried with vacuum. The extract was eluted with 12 mL of methanol and finally concentrated to 1 mL under a stream of nitrogen.

Liquid chromatography

Liquid chromatographic separation was done with a Waters Acquity UPLC using a Waters Acquity UPLC HSS T3 column (1.8 μm, 2.1x100 mm). For positive ion mode the eluent A was 5% methanol/water with 0.1% formic acid and eluent B was 100% methanol with 0.1% formic acid. For negative ion mode the eluent A was 5% methanol/water with 1 mM ammonium fluoride (NH_4F) and eluent B was 100% methanol with 1 mM ammonium fluoride (NH_4F). Gradient elution was used for both modes: 1 min 100% A, 30 min from 100% A to 100% B, 8 min 100 % B, and 3 min 100% A. The flow rate used was 0.2 mL/min and the injection volume 20 μL.

Mass spectrometry

The time-of-flight mass spectrometer was a Waters/Micromass LCT Premier XE with a dual electrospray (ESI) source. This source enables feeding of a lock mass solution (leucine encephaline) to be measured along the sample to correct for any mass errors during runs. The scan range was normally 60-800 m/z, the scan time was 0.09 s, and the interscan delay 0.01 s. The mass resolution of the spectrometer was typically about 12000 and the mass accuracy used in the identification was better than 5 ppm. The target

compounds were quantitated using the internal standard technique with isotope labelled standards. Caffeine (CFN), sulfamethoxazole (SMX), simazine (SMZ), carbamazepine (CBZ), atrazine (ATZ), and atenolol (ATN) were quantitated using positive ion mode and sucralose (SCL), diclofenac sodium salt (DCF), triclosan (TCS), and ibuprofen (IBP) using negative ion mode.

Diclofenac-13C6 sodium salt (Sigma-Aldrich), ibuprofen-d3 (Sigma-Aldrich), caffeine-13C3 (Sigma-Aldrich), carbamazepine-d10 (Sigma-Aldrich), estrone-2,4-d2 (CDN Isotopes), simazine-d10 (CDN Isotopes), triclosan-d3 (CDN Isotopes), atrazine-d5 (CDN Isotopes), sulfamethoxazole-d4 (CDN Isotopes), atenolol-d7 (TRC Canada) and sucralose-d6 (TRC Canada) were used as labelled standards for mass spectrometry analysis. The calibration was based on the same, non-labelled compounds.

Table S1. List of the 8 detected micropollutants and their physicochemical properties.
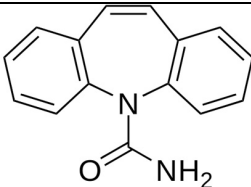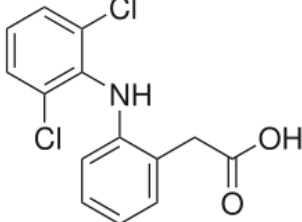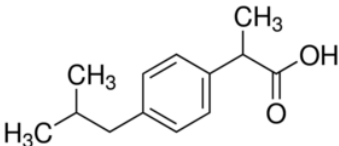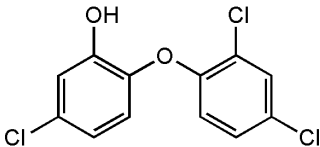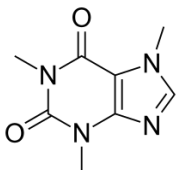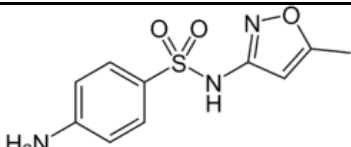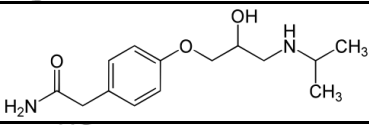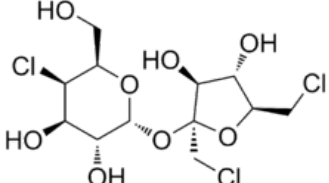
Compound	Molecular formula	Molecular mass (g mol^{-1})	pKa (-)	logK$_{ow}$ (-)
CBZ		236.3	13.9	2.28
DCF		296.1	4.15	4.48
IBP		206.3	4.9	3.37
TCS		289.5	7.8	5.12
CFN		194.2	0.5	0.28
SMX		253.3	5.81	0.65
ATN		266.34	9.6	0.16
SCL		397.63	12.52	0.229

Figure S1. *Escherichia coli* and *Enterococcus faecalis* inactivation in dark conditions (4 h) with different dosages of a) PMS; and b) PS.